Short Description of the 2-MGEM for the evaluation of pyrocarbon Anisotropy

G. E. Jellison

Oak Ridge National Laboratory

July 17, 2008

The principal application of the 2-MGEM to date is for the characterization of cross-sections of TRISO nuclear fuel (see Fig. 1) to be used in the advanced gas reactor (AGR) design, the 4th generation of nuclear power. The TRISO nuclear fuel particles are typically 800-1000 microns in diameter, and consist of 5 different layers. The central part is called the kernel, and is the radioactive part, usually consisting of uranium oxide and/or uranium carbide. The other 4 layers are deposited to encapsulate the radioactive kernel and to contain the kernel and any daughter nuclei resulting from the nuclear fission process. Because the 4th generation nuclear reactors are to be operated at much higher temperatures (~900 °C) than other reactor designs, the materials used in the 4 layers must be able to sustain these elevated temperatures. As a result, these layers are normally made of graphite and silicon carbide. The 4 layers of TRISO are: 1) the buffer, which is porous graphite, 2) the inner pyrocarbon (IPyC), 3) silicon carbide (SiC), and the outer pyrocarbon (OPyC) layer. The 2-MGEM measurements are used to characterize the optical anisotropy of the second and fourth layers pyrocarbon layers.

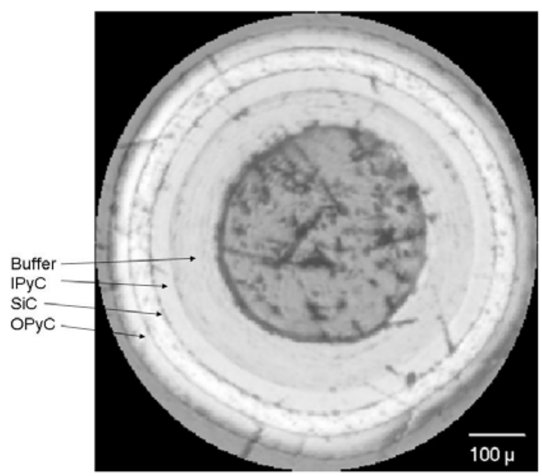

Figure 1: Light reflected intensity from a representative TRISO particle cross section. Each pixel measures ~2.5 microns in diameter.

It is well-known that graphite is a layered material with very strong inter-plane bonds and very weak intra-plane bonds. As a result, graphite is very highly optically anisotropic (ref. 1 and references therein). If highly oriented pyrolytic graphite (HOPG, the closest thing available to single crystal graphite) is cut and polished such that the graphene planes are perpendicular to the sample surface (or equivalently, the optic axis is in the sample surface plane), then light reflecting from this surface will see a large diattenuation N [defined as $N = (R_{max}-R_{min})/(R_{max}+R_{min})$, where R_{max}, R_{min} are the maximum and minimum reflectivities as a function of the polarization direction of the light, see refs. 2, 3). On the other hand, if the sample surface consists of amorphous carbon, diamond, or small graphite nanoparticles randomly oriented, then the diattenuation will be 0.

Therefore, the measurement of the diattenuation is also a measure of the preferential orientation of the graphite.

Figure 2 shows the raw 2-MGEM data (I_{Y0} and I_{Y1}), and the resultant diattenuation (N) and direction of principal axis (γ) for the TRISO cross section shown in Fig. 1. Both the IPyC and OPyC show much larger diattenuations than the buffer or SiC layers, but the diattenuation is far from being uniform. This non-uniformity is not noise-related, and comes from microscopic variations in the sample surface diattenuation. Because of the large amount of data obtained for each of the layers (>6000 points), statistical analysis can be performed. From the data of Fig. 2, the diattenuation of the IPyC and OPyC are 0.0101 and 0.0114 respectively, with standard deviations of 0.0061 and 0.0046. The average error of each point is <0.001.

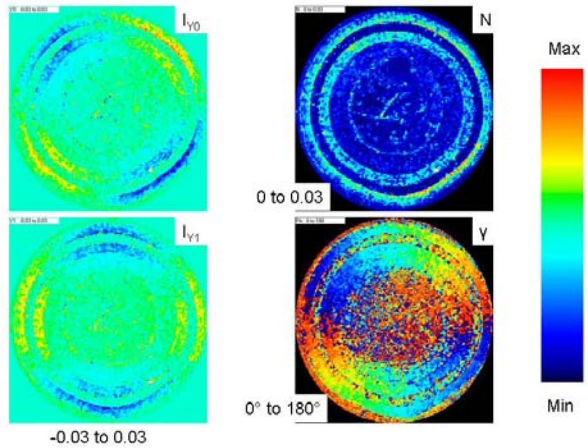

Figure 2. Images of the raw data (I_{Y0} and I_{Y1}) from the 2-MGEM measurement, the resulting diattenuation (N) and direction of the principal axis γ. The color scale is shown to the right with the maximum and minimum numbers shown in the figure.

Description of the 2-MGEM:

The two-modulator generalized ellipsometry microscope (2-MGEM) measures 8 elements of the Mueller matrix in reflection at near-normal incidence of a sample spot <4 microns in diameter [refs. 4-6]. For non-depolarizing samples, this information is sufficient to completely characterize the light polarization properties of the sample. Moreover, the accuracy of the individual components of the sample Mueller matrix is typically 0.001-0.002, making it far more accurate than competing techniques.

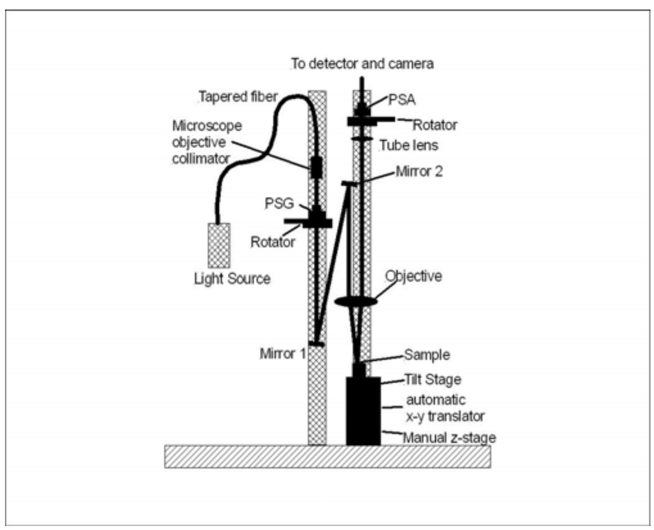

Figure 3 Schematic diagram of the reflection two-modulator generalized ellipsometer microscope (2-MGEM).

Figure 3 shows a schematic of the 2-MGEM. Incident light passes through the polarization state generator (PSG), which consists of a polarizer-photoelastic modulator (PEM) pair (oscillating at ~50 kHz). The PSG dynamically elliptically polarizes the light beam, where the ellipticity of the light polarization changes at the oscillating frequency of the PEM and includes linear, circular and elliptical polarization states. This polarized light beam then reflects off two aluminum mirrors and passes through a large diameter objective (acting as the condenser) before interacting with the sample. The light reflected from the sample then passes through the same large diameter objective (now acting as the objective) and through the polarization state analyzer (PSA). Like the PSG, the PSA consists of a PEM-polarizer pair, but where the oscillation frequency is now ~60 kHz rather than 50 kHz. Imaging optics are used to image the sample surface onto the CCD array detector and onto the pinhole before the photomultiplier tube (PMT, see Fig. 2). The CCD array is used only for sample positioning, while the light intensity at the PMT is converted to a voltage that is digitized and read into the computer. Imaging is accomplished by rastering the sample using a two-axis stage.

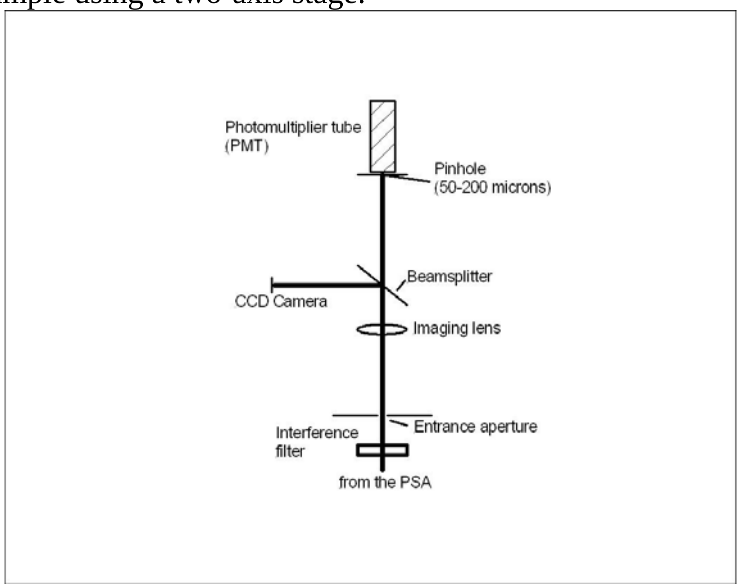

Figure 4: Detector and CCD camera configuration of the 2-MGEM.

The PMT current conversion to a voltage is accomplished by a specially designed electronic circuit, where the output dc current is held constant by dynamically changing the bias voltage on the PMT. This greatly simplifies the digitization electronics. The digitized signal is then analyzed using a Fourier-like integration procedure (see refs. 4, 5) that extracts 8 sample Mueller matrix elements from the waveform. These 8 parameters can then be further reduced to the diattenuation (N), the optical retardation (δ), the direction of the optical axis (γ), the circular diattenuation (CD), and the polarization factor (β). The most important parameter for this application is the optical diattenuation N, which is related to the traditional OPTical Anisotropy Factor (OPTAF) where OPTAF = $R_{max}/R_{min} = (1+N)/(1-N)$. OPTAF is the typically specified value used for fuel product acceptance by the nuclear industry.

Key Features

The 2-MGEM technique offers several advantages to all of the older techniques used in the past. In particular,

1) No sample rotation is needed.

2) 2-MGEM data is taken as a function of x- and y- position, making it possible to construct an image of the various measured parameters. Previous techniques were only able to measure at a single point.
3) The 2-MGEM measures 8 parameters, which then can be reduced to the diattenuation N and the principal direction γ. The quantities N and γ cannot be measured simultaneously using any of the older techniques above.
4) The 2-MGEM measures each of the 8 parameters to ~0.001; previous measurements of OPTAF were accurate to ~0.01. The 2-MGEM is 10 times more accurate.
5) The 2-MGEM can also measure retardation δ, circular diattenuation CD and the polarization factor β. These parameters are not measurable using the older techniques above, since those techniques do not incorporate a compensating optical element.

Product improvements for TRISO characterization

The previous older techniques were all developed in the 1970's for the characterization of the pyrocarbon layers in TRISO fuel. However, it was recognized that the results were inconsistent and not very reproducible. In a 1979 report discussing optical characterization of the pyrocarbon layers in TRISO nuclear fuels (ref. 7), Stevens stated:

> "The optical methods used were independently developed at several laboratories, and these methods have not been standardized. Consequently, the interrelationship between the measurements made at different laboratories and the degree of correlation of these measurements with preferred crystallite orientation *[n.b. the diattenuation is a measure of the preferred crystallite orientation.*] are not known.
>
> It is clear that optical methods have the potential to provide adequately low experimental uncertainty. But the fact that these methods are sensitive to experimental conditions will lead to very large uncertainties if adequate control of these conditions is not employed. …
>
> There are many consequences of large experimental uncertainty. For the HTGR [High Temperature Gas Reactor] application, these consequences generally fall into three categories:
>
> 1. The inability to systematically relate preferred orientation to irradiation performance. This limits the value of the optical method as a research tool.
> 2. The inability to systematically relate preferred orientation to deposition process conditions. This limits the value of the method as a process control tool.
> 3. Poor acceptance/rejection efficiencies. This limits the value of the method as a quality control tool.

Experience with using the 2-MGEM technique for measuring the optical diattenuation in pyrocarbon layers of prototype coated particle fuel has already shown that items #2 and #3 above can be adequately addressed using the 2-MGEM (see ref. 9), and experiments are now underway to address #1. Furthermore, our one installed instrument (at the Institute for Transuranic Elements (ITU) in Karlsruhe, Germany) has been used to measure a TRISO fuel particle that had previously been measured on the original instrument at Oak Ridge; both measured an average diattenuation of 0.0169.

References:

1. G. E. Jellison, Jr., J. D. Hunn, and H. N. Lee, “Measurement of optical functions of highly oriented pyrolytic graphite in the visible,” *Phys. Rev. B* **76**, 085125 (2007).
2. G. E. Jellison, Jr., and J. D. Hunn, “Optical anisotropy measurements of TRISO nuclear fuel particle cross-sections: the method,” *J. Nucl. Mater* **372** 36-44 (2008).
3. G. E. Jellison, Jr., J. D. Hunn, and R. A. Lowden, “Optical characterization of TRISO fuel particle cross-sections using generalized ellipsometry,” *J. Nucl. Mater.* **352** , 6-12, (2006).
4. G. E. Jellison, Jr. and F. A. Modine, “Two-Modulator Generalized Ellipsometry: Experiment and Calibration,” *Appl. Opt.* **36**, 8184-8189 (1997).
5. G. E. Jellison, Jr. and F. A. Modine, “Two-Modulator Generalized Ellipsometry: Theory,” *Appl. Opt.* **36**, 8190-8198 (1997).
6. G. E. Jellison, Jr., J. D. Hunn, and C. M. Rouleau, “Normal-incidence generalized ellipsometry using the two-modulator generalized ellipsometry microscope (2-MGEM)”, *Appl. Opt.***45**, 5479-5488 (2006)**.**
7. D. W. Stevens, “Optical anisotropy and preferred orientation in nearly isotropic pyrocarbons,” General Atomics Report number GA-A13307 (1975).
8. D. W. Stevens, “Round robin optical measurements of preferred orientation in nearly isotropic pyrocarbon,” General Atomics Report number GA-A15291 (1979).
9. J. D. Hunn, G.E. Jellison Jr., and R.A. Lowden, "Increase in pyrolytic carbon optical anisotropy and density during processing of coated particle fuel due to heat treatment," *J. Nucl. Mater.* (2008) in press.